

# Improved Arsenic Doping in Metalorganic Chemical Vapor Deposition of HgCdTe and *in situ* Growth of High Performance Long Wavelength Infrared Photodiodes

P. MITRA, Y.L. TYAN, and F.C. CASE

Loral Vought Systems Corporation, Dallas, TX 75265-0003

R. STARR and M.B. REINE

Loral Infrared and Imaging Systems, Lexington, MA 02173-7393

Controlled and effective p-type doping is a key ingredient for *in situ* growth of high performance HgCdTe photodiode detectors. In this paper, we present a detailed study of p-type doping with two arsenic precursors in metalorganic chemical vapor deposition (MOCVD) of HgCdTe. Doping results from a new precursor *tris*-dimethylaminoarsenic (DMAAs), are reported and compared to those obtained from tertiarybutylarsine (TBAs). Excellent doping control has been achieved using both precursors in the concentration range of  $3 \times 10^{15}$ – $5 \times 10^{17} \text{ cm}^{-3}$  which is sufficient for a wide variety of devices. Arsenic incorporation efficiency for the same growth temperature and partial pressure is found to be higher with DMAAs than with TBAs. For doping levels up to  $1 \times 10^{17} \text{ cm}^{-3}$ , the alloy composition is not significantly affected by DMAAs. However, at higher doping levels, an increase in the x-value is observed, possibly as a result of surface adduct formation of DMAAs dissociative products with dimethylcadmium. The activation of the arsenic as acceptors is found to be in the 15–50% range for films grown with DMAAs following a stoichiometric anneal. However, a site transfer anneal increases the acceptor activation to near 100%. Detailed temperature dependent Hall measurements and modeling calculations show that two shallow acceptor levels are involved with ionization energies of 11.9 and 3.2 meV. Overall, the data indicate that DMAAs results in more classically behaved acceptor doping. This is most likely because DMAAs has a more favorable surface dissociation chemistry than TBAs. Long wavelength infrared photodiode arrays were fabricated on P-on-n heterojunctions, grown *in situ* with iodine doping from ethyl iodide and arsenic from DMAAs on near lattice matched CdZnTe (100) substrates. At 77K, for photodiodes with 10.1 and 11.1  $\mu\text{m}$  cutoff wavelengths, the average (for 100 elements  $60 \times 60 \mu\text{m}^2$  in size) zero-bias resistance-area product,  $R_0A$  are 434 and 130  $\text{ohm}\cdot\text{cm}^2$ , respectively. Quantum efficiencies are  $\geq 50\%$  at 77K. These are the highest  $R_0A$  data reported for MOCVD *in situ* grown photodiodes and are comparable to state-of-the-art LPE grown photodiodes processed and tested under identical conditions.

**Key words:** Arsenic doping, HgCdTe, metalorganic chemical vapor deposition (MOCVD), photodiodes, tertiarybutylarsine, *tris*-dimethylaminoarsenic

## INTRODUCTION

A key requirement for *in situ* growth of bandgap engineered  $\text{Hg}_{1-x}\text{Cd}_x\text{Te}$  devices by vapor phase epitaxy is the ability to extrinsically dope with stable donor and acceptor dopants. The doping levels need to be precisely controlled and doping profiles precisely

positioned with respect to heterostructures involving different x-values. Furthermore, the donor and acceptor impurity atoms need to be located at the correct lattice sites to be fully active. In metalorganic chemical vapor deposition (MOCVD) of HgCdTe by the interdiffused multilayer process (IMP), we have demonstrated excellent control in iodine donor doping with ethyl iodide (EI).<sup>1</sup> The favorable dissociation chemistry of EI and low diffusivity of iodine allow

(Received December 30, 1995; revised April 22, 1996)

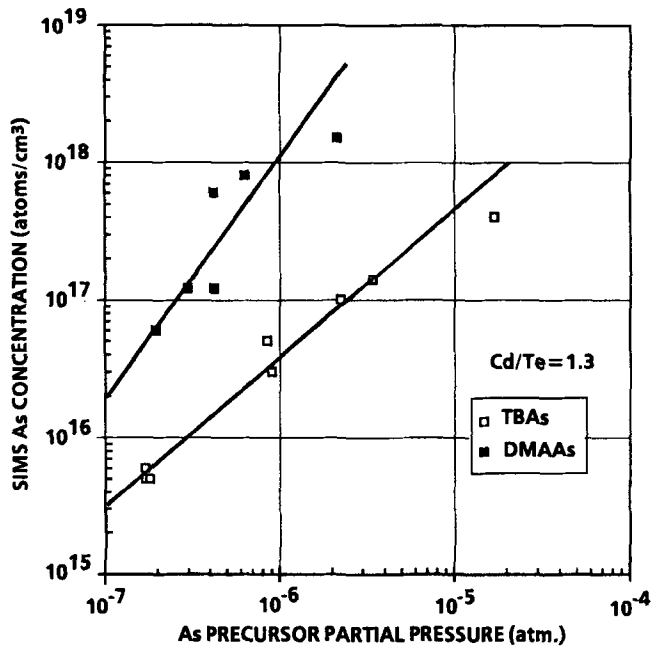


Fig. 1. SIMS As concentration data as a function of TBAs and DMAAs partial pressures. The Cd/Te ratio was maintained at 1.3 and other growth conditions were essentially the same in all of these runs.

abrupt I-profiles while avoiding the problems of memory effects with In precursors due to their reactivity with the Te-precursors. I-doped HgCdTe films have been shown<sup>1</sup> to exhibit electrical properties and lifetimes comparable to those of state-of-the-art In-doped HgCdTe films grown by liquid phase epitaxy (LPE).

For stable acceptor doping of HgCdTe for photodiode applications, arsenic is the most widely used dopant. In MOCVD, the precursors used for As-doping have been arsine and a number of substituted arsines. Of these, the substituted arsines tertiary-butylarsine (TBAs)<sup>2-7</sup> and phenylarsine<sup>8</sup> have been the most widely used recently since they are liquid sources at ambient temperatures and are safer alternatives to arsine. In MOCVD-IMP, good control in As-doping with TBAs has been obtained<sup>3,6</sup> over the range of  $3 \times 10^{15}$ – $5 \times 10^{17}$  cm<sup>-3</sup>. We have reported *in situ* growth and the characteristics of long wavelength infrared (LWIR) and medium wavelength infrared (MWIR) HgCdTe homojunction and heterojunction photodiodes<sup>6,7</sup> as well as independently accessed back-to-back MWIR/LWIR dual-band photodiode<sup>9</sup> detectors, using TBAs as the As precursor.

In previous work,<sup>7</sup> we have demonstrated that lifetimes at 80K of As-doped MOCVD HgCdTe with TBAs were always below the radiative limit. With a new precursor, *tris*-dimethylaminoarsenic (DMAAs) however, the corresponding As-doped material exhibited lifetimes<sup>7,10</sup> at the radiative limit and comparable to those achieved in Hg-rich LPE grown HgCdTe.<sup>11</sup>

There are important differences between the TBAs and DMAAs precursors which influence As-doping of HgCdTe. TBAs or  $\{CH_3\}_3CAsh_2$  is an arsine based precursor where one -H from AsH<sub>3</sub> has been substituted with the tertiarybutyl group. Clerjaud et al.<sup>12</sup>

have shown that As-doping of CdTe with AsH<sub>3</sub> causes the incorporation of As-H pairs in addition to As. Since As incorporation from TBAs in MOCVD-IMP HgCdTe occurs in an analogous manner, where TBAs is injected during the CdTe growth cycle, it is conceivable that similar As-H complexes are incorporated. Although the As-H complexes are expected to be electrically neutral, they are likely to be recombination centers in the HgCdTe and thus cause the lifetimes to be reduced. In a P-on-n heterojunction their presence in the critical depletion region would thus be detrimental and adversely affect the performance of the photodiodes.

A key reason for our choice of the DMAAs (or  $\{CH_3\}_2N\}_3-As$ ) precursor is that it has no As-H bonds and therefore it is expected that As-H complexes will not be incorporated in the As-doped films. The improved lifetime results<sup>7,10</sup> with DMAAs are consistent with this expectation. In our initial study of LWIR P-on-n heterojunctions grown *in situ* with DMAAs we have shown<sup>7</sup> that the photodiodes exhibited characteristics which are at least comparable to the best grown with TBAs. DMAAs also is a more convenient precursor for As-doping of HgCdTe since its vapor pressure (0.96 Torr at 15°C) is two orders of magnitude lower than that of TBAs at 15°C. Standard bubbler operation is thus possible with DMAAs instead of double dilution injection required with TBAs for controlled As-doping.<sup>6,7</sup>

In this paper, we describe a detailed study of As-doping with DMAAs of HgCdTe films grown on near lattice matched CdZnTe (100) substrates. The issues related to the chemical incorporation of As are addressed as well as its activation efficiency as an acceptor. Detailed Hall measurements on homogeneously doped epilayers are reported and the data are modeled to determine the acceptor ionization energy. In specific areas, the results are compared with As-doping using TBAs. Finally, new results on photodiode detector performance of LWIR P-on-n heterojunctions, grown *in situ* with DMAAs are reported. These mesa etched photodiode arrays were fabricated in a 64 × 64 array configuration with backside illumination. The characteristics of the MOCVD *in situ* grown photodiodes are compared to state-of-the-art LPE grown double layer heterojunction photodiodes fabricated and tested under identical conditions.

## EXPERIMENTAL APPROACH

The MOCVD-IMP growth of HgCdTe films was performed on lattice matched CdZnTe (nominally 3–5% Zn) substrates at 360°C. In most of this work, the orientation used was (100)4° toward the nearest (111) but some experiments were performed on the (211)B orientation as well. No significant differences were found in the As incorporation in (100) vs the (211)B oriented films. A horizontal geometry reactor system was used with elemental Hg and standard organometallic sources for Cd and Te, dimethylcadmium (DMCd) and diisopropyltelluride (DiPTe). The source precursors

sors were injected into the reactor through a single fast-switching manifold. Additional details of the growth system and the conditions used have been described previously.<sup>6,7</sup> For As-doping with TBAs, the bubbler was operated in a dual-dilution flow configuration allowing the TBAs partial pressure to be controlled in the range of  $2 \times 10^{-8}$ – $5 \times 10^{-5}$  atm. The DMAAs bubbler was operated under standard conditions and its partial pressure was varied in the range of  $5 \times 10^{-8}$ – $3 \times 10^{-6}$  atm. The As-precursor was injected into the reactor during the CdTe growth cycle since the Cd/Te ratio can be easily controlled. The Cd/Te ratio was varied from 1.0 to 1.5 to study the effect of this ratio on As incorporation.

To analyze the chemical incorporation levels of As and to determine the depth profiles, secondary ion mass spectrometry (SIMS) was employed with  $\text{Cs}^+$  ion bombardment. The SIMS depth profile measurements were performed at Charles Evans and Associates of Redwood City, CA. Detailed Hall effect measurements were performed as a function of temperature in the range of 300–10K. A magnetic field of 50 kGauss was used to ensure that the effect of residual donors were minimized.

P-on-n heterojunction films were grown *in situ* with the n-type region doped with I at  $(1-2) \times 10^{15} \text{ cm}^{-3}$  and the p-type cap doped with As at  $(1-3) \times 10^{17} \text{ cm}^{-3}$ . For I and As doping, EI and DMAAs were used, respectively. The n-type regions were grown to thicknesses of 14–16  $\mu\text{m}$  and the p-type caps were 2–3  $\mu\text{m}$ . The films were subjected to As site transfer activation and stoichiometric anneals as described previously.<sup>7</sup>

### ARSENIC INCORPORATION RESULTS

SIMS measurements were performed for HgCdTe (nominally  $x \sim 0.30$ ) layers doped using TBAs and DMAAs at various partial pressures. The data are plotted in Fig. 1 for epilayers grown with both precursors at Cd/Te ratio of 1.3. The data clearly indicate that for a given precursor partial pressure As-incorporation from DMAAs is significantly higher than from TBAs, by a factor of 7 to 20, with increasing partial pressure. This occurs at least in part due to the higher dissociation of DMAAs<sup>13</sup> (~50%) than TBAs<sup>14</sup> (~10%) at the MOCVD growth temperature of 360°C.

In Fig. 2, the SIMS depth profile data of a HgCdTe film with two As-doped regions from TBAs and DMAAs are shown. The DMCd and DiPTe partial pressures were kept the same and the Cd/Te ratio maintained at 1.3 during the entire growth run. The TBAs and DMAAs partial pressures were adjusted to  $2.2 \times 10^{-6}$  and  $3.0 \times 10^{-7}$  atm., respectively, which produced equivalent As concentration of  $1.2 \times 10^{17} \text{ atoms-cm}^{-3}$ . Thus, to achieve this As concentration, a factor of about 7.3 greater partial pressure of TBAs is required as compared to that of DMAAs. Also shown in Fig. 2, is the composition depth profile as determined from the  $^{125}\text{Te}$  secondary negative ion yield, which has been demonstrated to be a sensitive relative measure of the Cd mole fraction.<sup>15</sup> The absolute Cd mole fraction of the layer was determined from IR transmission mea-

surements to be 0.29. An increase in the Cd mole fraction due to the injection of the As-precursors is found to be small at  $\Delta x < 0.002$  under these doping conditions. This is an important result since it shows that the As incorporation and the HgCdTe alloy composition can be independently controlled for doping levels  $\leq 1.2 \times 10^{17} \text{ cm}^{-3}$  under the growth conditions used in the present experiments. Some diffusion of As is observed to occur for As introduced from both sources which may be due to a small percentage of the As atoms incorporated into the metal sublattice sites.

The effect of higher levels of DMAAs injection on As-incorporation and x-value was studied by growing a layer with two As-doped regions with DMAAs partial pressures of  $4.2 \times 10^{-7}$  and  $2.1 \times 10^{-6}$  atm. The DMCd and DiPTe partial pressures were kept the same and the Cd/Te ratio was maintained at 1.3 throughout the growth run. The SIMS As and  $^{125}\text{Te}$  depth profiles are shown in Fig. 3. The doping levels obtained at the two partial pressures are  $6 \times 10^{17}$  and  $1.6 \times 10^{18} \text{ atoms-cm}^{-3}$ . Thus, for a factor of 5 higher DMAAs partial pressure, an increase of only a factor of 2.7 in As concentration is obtained. Clearly, in this regime As-incorporation does not increase linearly with increasing DMAAs partial pressures and begins to saturate. Figure 3 also shows that at the lower DMAAs injection only a very small change in x-value occurs, but at higher injection of  $2.1 \times 10^{-6}$  atm there is a substantial increase in the Cd mole fraction with  $\Delta x = 0.08$ .

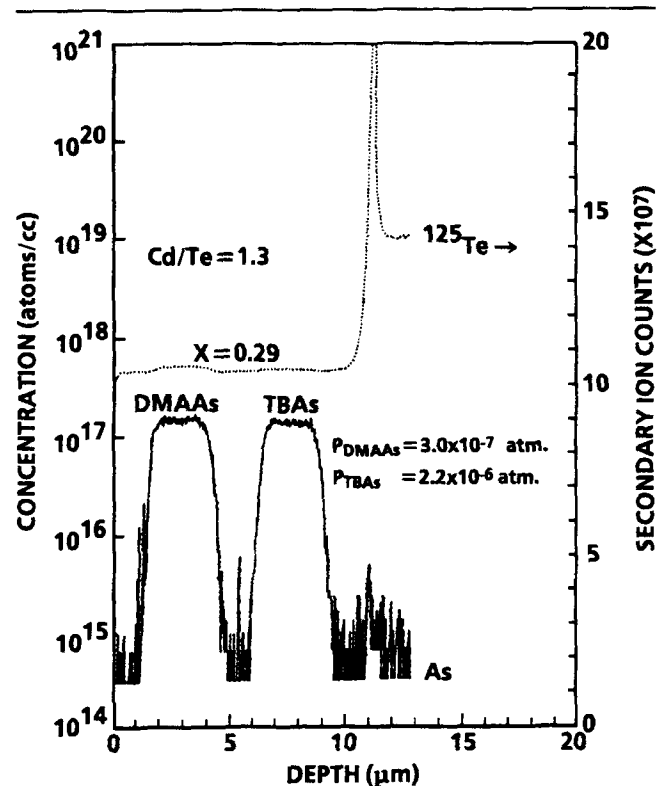


Fig. 2. SIMS depth profiles of As concentration and the  $\text{Hg}_{1-x}\text{Cd}_x\text{Te}$  x-value for doping with TBAs and DMAAs at partial pressures of  $2.2 \times 10^{-6}$  and  $3.0 \times 10^{-7}$  atm., respectively. Except for switching the As-precursors on and off, no other changes were made during the growth run.

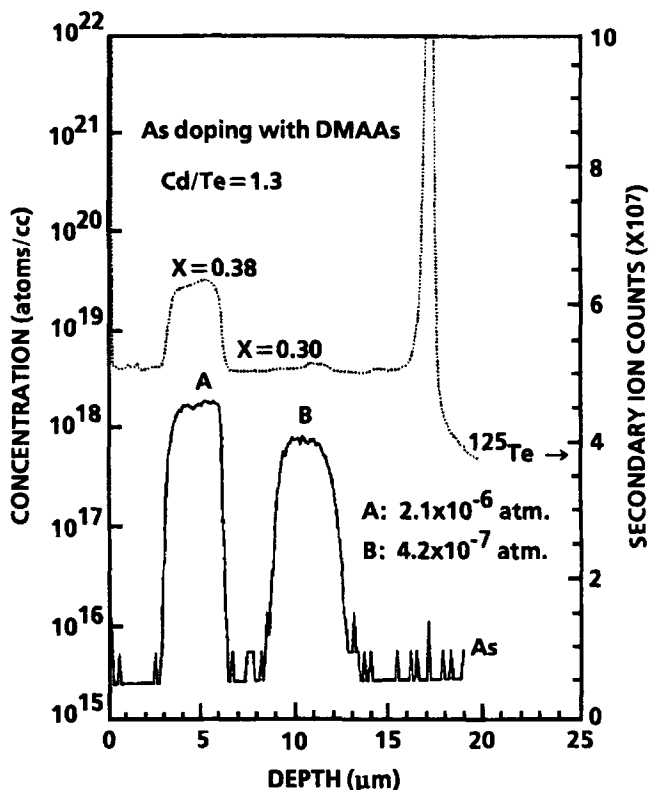


Fig. 3. SIMS depth profiles of As concentration and the  $Hg_{1-x}Cd_xTe$   $x$ -value for doping with DMAAs at partial pressures of  $4.2 \times 10^{-7}$  and  $2.1 \times 10^{-6}$  atm. The Cd/Te ratio was maintained at 1.3 and except for switching the DMAAs on and off no other changes were made during the run.

The influence of As-doping with TBAs on the HgCdTe alloy composition in MOCVD-IMP has been reported by Bubulac et al.<sup>15</sup> These authors observed an increase in the Cd mole fraction with  $\Delta x = 0.115$  for an As-doping level of  $2 \times 10^{17} \text{ cm}^{-3}$ . This is a much larger change in composition than in the present work with TBAs shown in Fig. 2 and may be related to the differences in the exact details of the growth conditions. The increase in the  $x$ -value with As doping is quite likely due to adduct formation of TBAs or a dissociated As containing product with DMCD on the CdTe surface resulting in increased Cd incorporation. The adduct formation weakens the  $CH_3$ -Cd bond and quite likely makes the surface DMCD dissociation more kinetically favored over desorption. With DMAAs also, in addition to unimolecular dissociation, adduct formation occurs with DMCD on the film surface quite possibly with partially dissociated DMAAs. At low injection rates, the chemical incorporation of As varies linearly, but at high injection second or higher order reaction kinetics are clearly evident.

In their experiments on As-doping with  $AsH_3$  in MOCVD-IMP, Capper et al.<sup>16</sup> found that As was selectively incorporated in the CdTe layers only. It was reported that  $AsH_3$  forms an adduct with DMCD, even at room temperature, and the pyrolysis of the adduct at the 410°C growth temperature resulted in the incorporation of As in the CdTe layer.  $AsH_3$  is not expected to pyrolyze at this temperature. It was noted

that at Cd/Te ratio of 0.8 an increase in HgTe growth rate was observed which resulted in a reduction in  $x$ -value. Upon increasing the Cd/Te to 1.2, the change in composition was not significant, however, the associated doping level was not reported. In direct alloy growth of HgCdTe both for As-doping with  $AsH_3$ <sup>17</sup> and TBAs,<sup>5</sup> a reduction in  $x$ -value was reported when either of the precursors were injected under otherwise similar growth conditions. This composition change was also attributed to adduct formation of the As-precursor to DMCD in the gas phase.

The mechanism of As-incorporation with the precursors used in the present work is distinctly different from As-doping with  $AsH_3$ . A key difference is that  $AsH_3$  does not pyrolyze by itself at the HgCdTe growth temperature whereas both TBAs and DMAAs pyrolyzes albeit to different degrees. DMAAs starts to decompose at 250°C, is 50% converted at 350°C and thermal decomposition is complete at 450°C.<sup>13</sup> TBAs, by comparison, starts to decompose at 350°C is 50% converted at 380°C and full dissociation is not achieved even at 550°C.<sup>14</sup> The bond dissociation energies for the three As precursors follow the order  $As-H > As-C > As-N$ . Thus, incorporation of As from DMAAs is expected to be most efficient. The thermal decomposition temperatures for DMAAs suggest that the results shown in Fig. 3 for As incorporation at 360°C are consistent with both unimolecular thermal decomposition, which occurs at low injection rates, as well as surface-adduct formation of As containing partially dissociated products of DMAAs with DMCD at high injection rates resulting in increased  $x$ -values. The two incorporation pathways are expected to be kinetically competitive and will probably be significantly altered with relatively small changes in growth temperatures.

#### ACTIVATION OF ARSENIC AS ACCEPTORS

The efficient incorporation of As in HgCdTe does not necessarily indicate that As atoms are active as acceptors. In fact, the amphoteric nature of As in HgCdTe is well established<sup>18</sup> and for the As to behave as an acceptor it must substitutionally occupy the Te-sublattice sites. To determine the degree of acceptor activation of the As from DMAAs several homogeneously As-doped films were analyzed by SIMS concentration and Hall measurements at 80K. The film thicknesses were typically 9–12 μm. Hall measurements were performed on a section of each film which underwent a stoichiometric anneal only and another section of the same film which underwent both an activation and a stoichiometric anneal. The activation anneal was performed at 415°C and the stoichiometric anneal at 235°C both under saturated Hg pressures. In Fig. 4, the measured Hall concentrations ( $1/eR_H$ , where  $R_H$  is the Hall coefficient) for both annealing conditions are plotted as a function of the SIMS As-concentration.

Figure 4 shows that when the films are subjected to a stoichiometric anneal only the acceptor activation is generally low varying from 15–50%. At the lower As-

concentrations, below  $1 \times 10^{17} \text{ cm}^{-3}$ , the activation is <25% increasing to 50% at higher concentrations. The same films after the activation and stoichiometric anneals exhibit Hall concentrations which are significantly higher and close to 100% acceptor activation. These data indicate that in the as-grown films at the lower doping levels, the majority of the As atoms do not substitutionally occupy the Te-sublattice sites despite a Cd/Te ratio  $>1$ . At higher doping levels, the probability increases to 50%. The activation anneal causes an effective site transfer of the As-atoms to the Te-sublattice resulting in their behaving as acceptors. The conditions for the activation anneal in this work was not optimized but are similar to that described previously<sup>7</sup> and for site transfer in As-implanted HgCdTe films.<sup>19</sup> It is conceivable that an effective site transfer could be performed at lower temperatures.

The acceptor activation data in Fig. 4 also corroborate the inferences made from Figs. 2 and 3 that at low concentrations very little adduct formation with DMCD occurs (no change in  $x$ -value) and consequently the As does not necessarily get substitutionally incorporated in the Te-sublattice. However, at the higher DMAAs injection rates surface adduct formation becomes important and therefore forces the As-atoms to occupy Te-sublattice sites. This results in the higher acceptor activation efficiency observed when the As concentrations are  $\geq 1 \times 10^{17} \text{ cm}^{-3}$ , prior to the site transfer activation anneal.

### HALL CHARACTERIZATION RESULTS

Hall measurements were performed on a large number of homogeneously As-doped HgCdTe films ( $x \sim 0.30$ ) with DMAAs. The Cd/Te ratios during growth were 1.2 and 1.5. The data reported here were all taken at 50 kGauss. The Hall data were taken after the films were subjected to an activation and a stoichiometric anneal. Film thicknesses were in the 9–12  $\mu\text{m}$  range. In Fig. 5, the 80K Hall concentrations are plotted as a function of the DMAAs partial pressure used during growth. The data clearly indicate that the incorporation of As acceptors is higher, at the higher Cd/Te ratio and that to achieve doping levels at  $\geq 3 \times 10^{17} \text{ cm}^{-3}$  a ratio of 1.5 is necessary. For controlled low doping levels of  $\sim 1 \times 10^{16} \text{ cm}^{-3}$ , however, the lower ratio of 1.2 is preferable.

Detailed temperature dependent Hall measurements from 300–10K were performed for As-doped HgCdTe using both TBAs and DMAAs. The measured mobility and carrier concentration ( $1/eR_H$ ) as a function of inverse temperature for two  $x = 0.30$  films are shown in Figs. 6a and 6b for TBAs and DMAAs, respectively. The two films have carrier concentrations ( $N_A - N_D$ ) at 80K that are closely comparable at  $1.82 \times 10^{16}$  and  $1.74 \times 10^{16} \text{ cm}^{-3}$ . Both show the expected carrier freezeout behavior but exhibit somewhat different temperature dependence. The data for the TBAs doped film suggest that more than one acceptor ionization energy is involved, in contrast to the DMAAs doped film for which the

inverse temperature dependence follows a single exponential and therefore involves a single ionization energy. Secondly, the 80K mobility for the TBAs doped film is lower with a value of  $241 \text{ cm}^2/\text{V-s}$  as compared to  $313 \text{ cm}^2/\text{V-s}$  for the DMAAs doped film with the same carrier concentration. At lower temperatures also the mobility of the film doped with DMAAs is higher than the one with TBAs. Thus, although both precursors produce p-type doping of HgCdTe, there are clear differences in the temperature dependence of the Hall data.

### MODELING OF HALL CONCENTRATIONS

The measured Hall carrier concentrations for four  $x = 0.30$  As-doped films with DMAAs are plotted vs

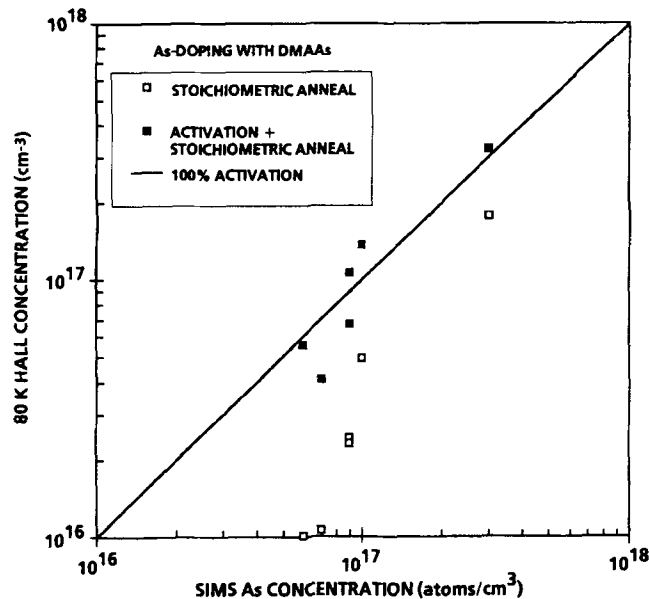


Fig. 4. Acceptor activation plot of 80K Hall concentration measured after stoichiometric anneal only and after activation plus stoichiometric anneals, vs SIMS As concentration for HgCdTe doped with DMAAs.

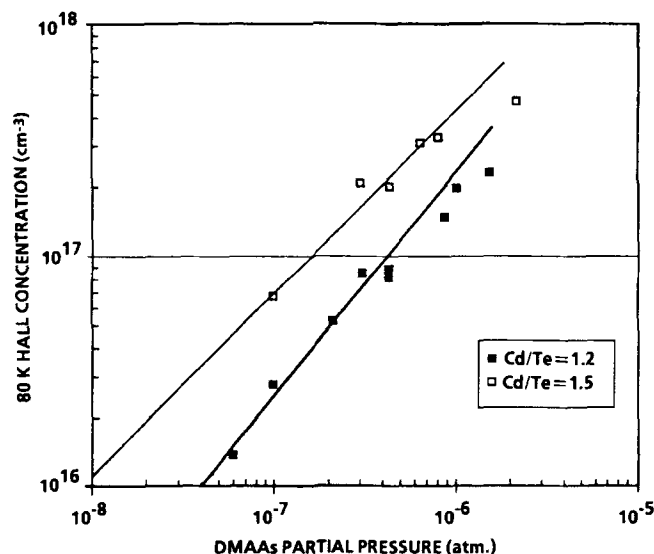


Fig. 5. Hall acceptor concentrations at 80K in several As-doped  $\text{Hg}_{0.70}\text{Cd}_{0.30}\text{Te}$  films grown with Cd/Te ratios of 1.2 and 1.5, plotted as a function of DMAAs partial pressures.

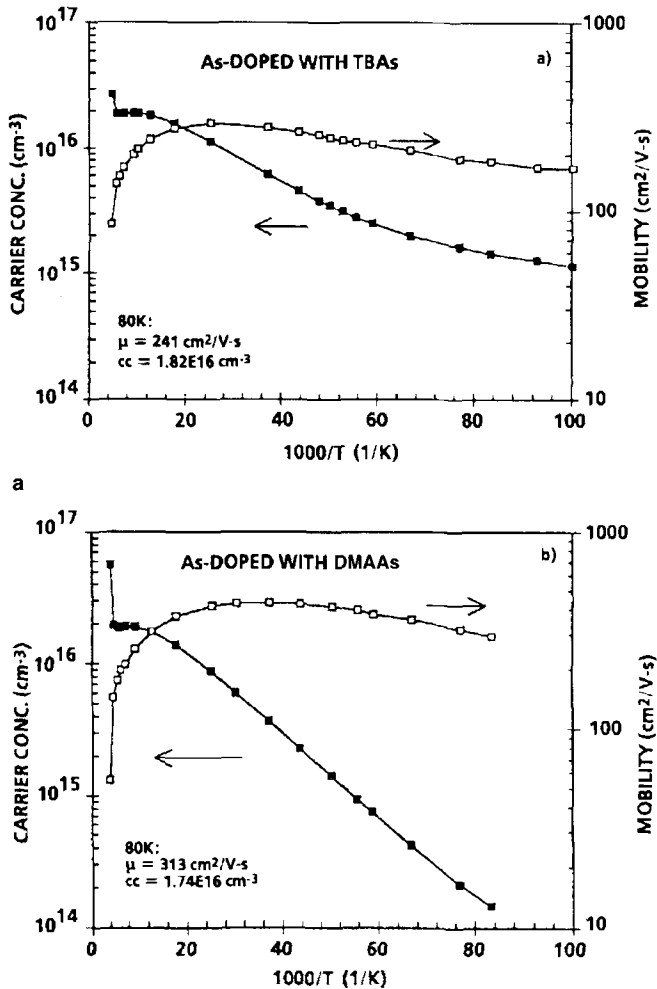


Fig. 6. Temperature dependence of Hall carrier concentration and mobility for As-doped Hg<sub>0.70</sub>Cd<sub>0.30</sub>Te films with (a) TBAs and (b) DMAAs. The Hall measurements were performed at 50 kGauss. The thicknesses of the films in (a) and (b) are 9.0 and 9.8 μm, respectively.

reciprocal temperature in Fig. 7. For low carrier concentrations,  $<1 \times 10^{17} \text{ cm}^{-3}$ , the freezeout behavior is pronounced but less so at higher concentrations. Also, except at the lowest carrier concentration ( $\sim 2 \times 10^{16} \text{ cm}^{-3}$  at 80K) the inverse temperature dependence of the  $\log(N_A - N_D)$  does not follow a straight line indicating that more than one ionization energy is involved. This behavior has previously been noted by Finkman and Nemirovsky<sup>20</sup> for both As-doped and Au-doped bulk HgCdTe crystals. These authors found that two acceptor levels were required to explain the temperature dependence accurately.

In this work, we have also used two shallow acceptor levels to model the Hall concentration data vs temperature and to determine the ionization energies. The activation energies  $E_{a1}$  and  $E_{a2}$  in meV for fitting the measured Hall data are:

$$E_{a1} = 1725.4 / \epsilon(x)^2 - [(1.158 \times 10^{-4}) / \epsilon(x)] (N_a^-)^{1/3} \quad (1)$$

$$E_{a2} = 467.5 / \epsilon(x)^2 - [(1.158 \times 10^{-4}) / \epsilon(x)] (N_a^-)^{1/3} \quad (2)$$

where the static dielectric constant  $\epsilon(x)$  as a function of  $x$ -value was determined from empirical relations,<sup>21</sup>

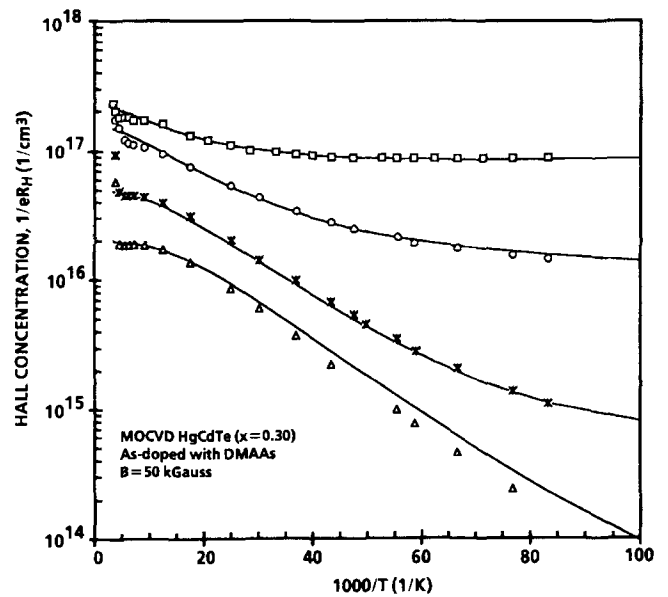


Fig. 7. Experimental (data points) and calculated (solid curves) temperature dependence of Hall carrier concentration for As-doped Hg<sub>0.70</sub>Cd<sub>0.30</sub>Te films with DMAAs for a range of As concentrations.

and where  $N_a^-$  is the number of ionized acceptors per unit volume. Equations (1) and (2) are identical in form to the commonly used expression<sup>22</sup> for single acceptor levels:

$$E_a = E_0 - \alpha(N_a - N_d)^{1/3} \quad (3)$$

The hole concentration  $p_0(T)$  as a function of temperature was computed from the following charge neutrality equation:

$$p_0 + N_d = N_{a1} / (1 + g \exp[(E_{a1} - E_f) / kT]) + N_{a2} / (1 + g \exp[(E_{a2} - E_f) / kT]) \quad (4)$$

where  $p_0$  is the hole concentration,  $N_{a1}$  and  $N_{a2}$  are the concentrations of the acceptors with activation energies  $E_{a1}$  and  $E_{a2}$ , respectively,  $E_f$  is the Fermi level and  $g$  is the degeneracy of the acceptor states and is assumed to be 4.

In Eq. (4),  $N_d$  is the free donor concentration, and in most DMAAs doped films a good fit for  $p_0(T)$  was obtained with  $N_d = 0$ . Since  $E_{a2}$  is much lower than  $E_{a1}$ ,  $N_{a2}$  is fully ionized at a much lower temperature than  $N_{a1}$ . Hence in computing  $E_{a1}$ ,  $N_{a2}$  is included in the concentration of the ionized acceptors.

In Fig. 7, the modeling results for the carrier concentration  $p_0(T)$  are overlaid on the measured Hall data. Except for the low acceptor concentration sample, the fits to the experimental data are excellent. For the low concentration sample, a single acceptor level description is sufficient; but at the higher concentrations, the inclusion of two acceptor levels is essential to fit the data.

In Fig. 8, the values of  $E_{a1}$  and  $E_{a2}$ , determined by the best fit of the calculated  $p_0(T)$  to the experimental Hall data, are plotted vs acceptor concentration for a number of As-doped  $x = 0.30$  films for which DMAAs was used. The solid lines are the fits using the two-level model described above and have the form:

$$E_{a1} = 11.94 - 9.63 \times 10^{-6} (N_{a1})^{1/3} \quad (5)$$

$$\text{and } E_{a2} = 3.23 - 9.63 \times 10^{-6} (N_{a2})^{1/3} \quad (6)$$

The concentration independent As-acceptor ionization energies  $E_{o1}$  and  $E_{o2}$  are thus 11.94 and 3.23 meV, respectively, for MOCVD HgCdTe with  $x = 0.30$ .

Kenworthy et al.<sup>23</sup> have reported an empirical expression for acceptor ionization energies in bulk HgCdTe doped with Cu, Ag, As, and Sb using a single acceptor level. Since this expression is not specifically derived from As-doped HgCdTe data alone, it can only provide a rough estimate of the ionization energy. Using their expression an ionization energy of 13.96 meV is estimated for  $x = 0.30$  HgCdTe. Kalisher<sup>24</sup> has determined  $E_o$  of 10.5 meV for As-doped HgCdTe ( $x = 0.20$ ) grown from Hg rich LPE. The present work is the first detailed analysis of ionization energies from MOCVD As-doped HgCdTe and are in the same range as those obtained from bulk and LPE material.

### PHOTODIODE RESULTS

P-on-n heterojunction films, grown *in situ* with DMAAs and EI precursors, were processed into backside-illuminated mesa etched  $64 \times 64$  photodiode arrays with CdTe passivation. The unit cell area was  $60 \times 60 \mu\text{m}^2$  and the junction area was  $35 \times 35 \mu\text{m}^2$ . Electrical measurements on selected photodiodes in each array were performed at 77K by making contact to each selected indium bump by a computer controlled mechanical probe. The center  $10 \times 10$  elements of each array were cryoprobed in this manner. The zero-bias resistance-area products  $R_o A_{OPT}$  were determined by using the optical area  $A_{OPT}$  of the junctions,  $60 \times 60 \mu\text{m}^2$ . The spectral responses, cutoff wavelengths, and quantum efficiencies were measured at 77K in the backside illuminated mode for selected elements of each array after it had been bump-interconnected to a  $64 \times 64$  Si CMOS readout chip.

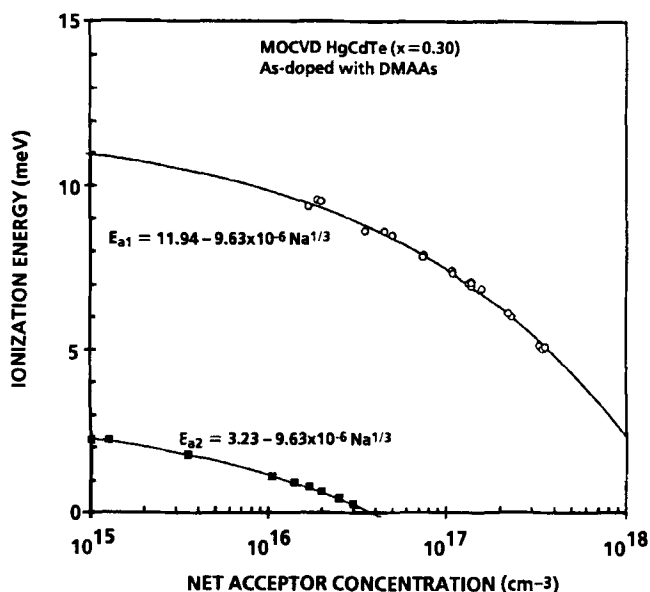


Fig. 8. Ionization energies of several As-doped  $\text{Hg}_{0.70}\text{Cd}_{0.30}\text{Te}$  films with DMAAs (data points) determined from the two-level fits shown in Fig. 7. The solid lines are from the two equations for  $E_{a1}$  and for  $E_{a2}$ .

The average  $R_o A_{OPT}$  value for the center  $10 \times 10$  elements of each  $64 \times 64$  array at 77K is plotted vs the measured cutoff wavelength at 77K in Fig. 9. Included in the plot are similar data from Loral's standard LPE grown HgCdTe arrays. The processing and the testing of the MOCVD and LPE grown arrays were performed under essentially identical conditions. Also shown in Fig. 9 is the theoretical calculation of  $R_o A$  vs cutoff wavelength at 77K, for n-side diffusion current and Auger limited lifetimes for  $n_o = 1 \times 10^{15} \text{ cm}^{-3}$ .

The measured  $R_o A_{OPT}$  data for the MOCVD films shown in Fig. 9 approach the diffusion limit calculations and show a trend identical to the LPE data. For photodiodes with 10.1 and 11.1  $\mu\text{m}$  cutoff wavelength, the average  $R_o A$  are 434 and 130  $\text{ohm}\cdot\text{cm}^2$ , respectively. These are the highest  $R_o A$  data reported to-date for MOCVD grown LWIR HgCdTe photodiodes. The average quantum efficiency of the MOCVD arrays are  $\geq 50\%$  and the spectral responses are classical. Additional details of the performance of the MOCVD photodiodes will be described elsewhere.

### SUMMARY AND CONCLUSIONS

In this paper, we have described a detailed study of arsenic doping in MOCVD-IMP HgCdTe with the new precursor DMAAs. Controlled As-doping in the range of  $1 \times 10^{16} - 5 \times 10^{17} \text{ cm}^{-3}$  was achieved. This doping range meets the requirements for most HgCdTe device applications. SIMS concentration measurements show that As is incorporated in a significantly more efficient manner from DMAAs than the previously and more widely used precursor, TBAs. As-doping from DMAAs can be controlled independently of any

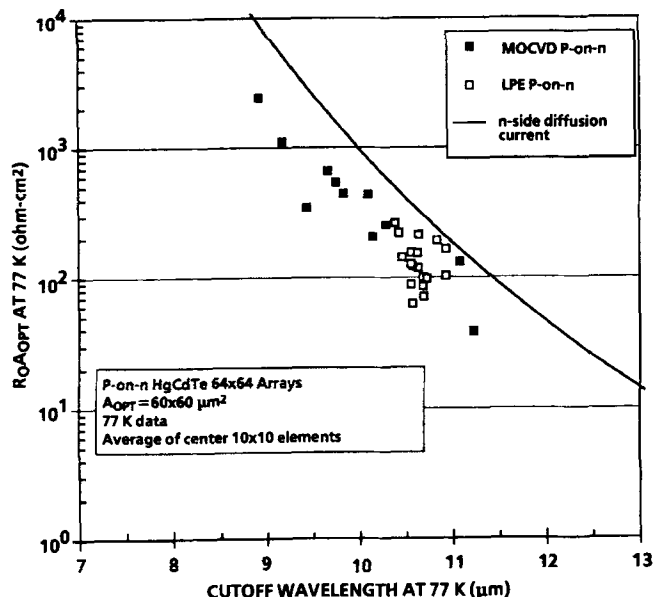


Fig. 9. 77K  $R_o A_{OPT}$  data for MOCVD P-on-n heterojunctions (filled squares) grown *in situ* with DMAAs for As-doping. Each data point is the average of the center 100 elements from a  $64 \times 64$  array. For comparison similar data from Loral's LPE grown junctions (empty squares) are included. Both types of films were processed and tested in an identical manner.

changes in the HgCdTe alloy composition when the doping level is  $1 \times 10^{17} \text{ cm}^{-3}$ . For higher doping levels, the concentration of As does not increase linearly with the DMAAs partial pressure, most likely due to surface adduct formation with DMAAs dissociative products. As a consequence, at high As concentrations the x-value of HgCdTe increases. For a doping level of  $6 \times 10^{17} \text{ cm}^{-3}$ , the change in x-value is negligibly small but at  $2 \times 10^{18} \text{ cm}^{-3}$  an increase with  $\Delta x = 0.08$  was observed.

As-grown, the As-doped films with DMAAs show only partial activation of acceptors. However, following a site transfer activation anneal, the As impurity exhibits near 100% activation. Detailed temperature dependent Hall effect measurements indicate that classical p-type characteristics are achieved. An analysis of the Hall data on  $x = 0.30$  HgCdTe show that two shallow acceptor levels with ionization energies of 11.94 and 3.23 meV are involved.

LWIR P-on-n heterojunction films grown with I-doped n-type regions and As-doped p-type caps with DMAAs have produced the highest  $R_0A$  values in MOCVD HgCdTe to-date. The present photodiode array data provides compelling evidence that DMAAs is a highly effective precursor for As-doping in MOCVD of HgCdTe. The results also demonstrate that the improvements in both donor and acceptor doping have contributed to advancing MOCVD to produce HgCdTe photodiodes of the same quality as that achieved from state-of-the-art LPE material at 77K.

#### ACKNOWLEDGMENTS

This work was supported by Loral internal research funds. We thank Dr. Lewis Claiborne for encouragement, helpful discussions, and comments on the manuscript. We are also grateful to Dr. Joseph P. Omaggio and James Waterman of the U.S. Naval Research Laboratory for many stimulating discussions and their keen interest in this work.

#### REFERENCES

1. P. Mitra, Y.L. Tyan, T.R. Schimert and F.C. Case, *Appl. Phys. Lett.* 65, 195 (1994).
2. D.D. Edwall, J.-S. Chen and L.O. Bubulac, *J. Vac. Sci. Technol. B* 9, 1691 (1991).
3. D.D. Edwall, L.O. Bubulac and E.R. Gertner, *J. Vac. Sci. Technol. B* 10, 1423 (1992).
4. J. Elliot and V.G. Kreismanis, *J. Vac. Sci. Technol. B* 10, 1428 (1992).
5. V. Rao, H. Ehsani, I.B. Bhat, M. Kestigian, R. Starr, M.H. Weiler and M.B. Reine, *J. Electron. Mater.* 24, 437 (1995).
6. P. Mitra, T.R. Schimert, F.C. Case, R. Starr, M.H. Weiler, M. Kestigian and M.B. Reine, *J. Electron. Mater.* 24, 661 (1995).
7. P. Mitra, T.R. Schimert, F.C. Case, S.L. Barnes, M.B. Reine, R. Starr, M.H. Weiler and M. Kestigian, *J. Electron. Mater.* 24, 1077 (1995).
8. C.D. Maxey, I.G. Gale, J.B. Clegg and P.A.C. Whiffin, *Semicond. Sci. Technol.* 8, S183 (1993).
9. M.B. Reine, P.W. Norton, R. Starr, M.H. Weiler, M. Kestigian, B.L. Musicant, P. Mitra, T. Schimert, F.C. Case, I.B. Bhat, H. Ehsani and V. Rao, *J. Electron. Mater.* 24, 669 (1995).
10. H.D. Shih, M.J. Bevan and M.C. Chen, presented at the 1995 U.S. Workshop Phys. and Chem. of Mercury Cadmium Telluride and Other IR Mater.
11. T. Tung, M.H. Kalisher, A.P. Stevens, P.E. Herning, *Mater. Res. Soc. Symp. Proc.* 90 (Pittsburgh, PA: Mater. Res. Soc., 1987), p. 321.
12. B. Clerjaud, D. Cote, L. Svob, Y. Marfaing and R. Druilhe, *Solid State Comm.* 85, 167 (1993).
13. S. Salim, J.P. Lu, K.F. Jensen and D.A. Bohling, *J. Cryst. Growth* 124, 16 (1992).
14. C.A. Larsen, N.I. Buchan, S.H. Li and G.B. Stringfellow, *J. Cryst. Growth* 94, 663 (1989).
15. L.O. Bubulac, D.D. Edwall, J.T. Cheung and C.R. Viswanathan, *J. Vac. Sci. Technol. B* 10, 1633 (1992).
16. P. Capper, C.D. Maxey, P.A.C. Whiffin and B.C. Easton, *J. Cryst. Growth* 97, 833 (1989).
17. N.R. Taskar, I.B. Bhat, K.K. Parat, S.K. Ghandhi and G.J. Scilla, *J. Vac. Sci. Technol. B* 9, 1705 (1991).
18. H.R. Vydyanath, *J. Vac. Sci. Technol. B* 9, 1716 (1991).
19. S.J.C. Irvine, J. Bajaj and L.O. Bubulac, *Mater. Res. Soc. Symp. Proc.* 299, (Pittsburgh, PA: Mater. Res. Soc., 1994), p. 99.
20. E. Finkman and Y. Nemirovsky, *J. Appl. Phys.* 59, 1205 (1986).
21. S. Roland, *Properties of Narrow Gap Cadmium-Based Compounds*, ed P. Capper, (London: INSPEC, IEE, 1994), EMIS Data Reviews, No. 10, p. 80.
22. J. Leloup, H. Djerassi and J.H. Albany, *J. Appl. Phys.* 49, 3359 (1978).
23. I.K. Kenworthy, P. Capper, C.L. Jones, J.J.G. Gosney and W.G. Coates, *Semicond. Sci. Technol.* 5, 854 (1990).
24. M.H. Kalisher, *J. Cryst. Growth* 70, 365 (1984).